Antisense oligonucleotide rescue of CGG expansion-dependent mis-splicing in fragile X syndrome restores FMRP

PNAS RESEARCH ARTICLE | NEUROSCIENCE

Antisense oligonucleotide rescue of CGG expansion–dependent *FMR1* mis-splicing in fragile X syndrome restores FMRP

Sneha Shah[a], Kevin J. Sharp[b], Sithara Raju Ponny[a], Jonathan Lee[c], Jonathan K. Watts[c,d,e], Elizabeth Berry-Kravis[b,f,g], and Joel D. Richter[a,e,1]

Edited by Michael Rosbash, Brandeis University, Waltham, MA; received February 16, 2023; accepted May 26, 2023

Aberrant alternative splicing of mRNAs results in dysregulated gene expression in multiple neurological disorders. Here, we show that hundreds of mRNAs are incorrectly expressed and spliced in white blood cells and brain tissues of individuals with fragile X syndrome (FXS). Surprisingly, the *FMR1 (Fragile X Messenger Ribonucleoprotein 1)* gene is transcribed in >70% of the FXS tissues. In all *FMR1*-expressing FXS tissues, *FMR1* RNA itself is mis-spliced in a CGG expansion–dependent manner to generate the little-known *FMR1*-217 RNA isoform, which is comprised of *FMR1* exon 1 and a pseudo-exon in intron 1. *FMR1*-217 is also expressed in FXS premutation carrier–derived skin fibroblasts and brain tissues. We show that in cells aberrantly expressing mis-spliced *FMR1*, antisense oligonucleotide (ASO) treatment reduces *FMR1*-217, rescues full-length *FMR1* RNA, and restores FMRP (Fragile X Messenger RibonucleoProtein) to normal levels. Notably, *FMR1* gene reactivation in transcriptionally silent FXS cells using 5-aza-2′-deoxycytidine (5-AzadC), which prevents DNA methylation, increases *FMR1*-217 RNA levels but not FMRP. ASO treatment of cells prior to 5-AzadC application rescues full-length *FMR1* expression and restores FMRP. These findings indicate that misregulated RNA-processing events in blood could serve as potent biomarkers for FXS and that in those individuals expressing *FMR1-217*, ASO treatment may offer a therapeutic approach to mitigate the disorder.

antisense oligonucleotides | *FMR1* | RNA splicing | FMRP

Significance

White blood cells from over 70% of fragile X syndrome (FXS) individuals express an aberrantly spliced *FMR1* transcript isoform called *FMR1-217* RNA. This isoform is also expressed in the FXS postmortem brain. *FMR1-217* RNA is rescued to the normally spliced *FMR1* RNA by treatment with antisense oligonucleotides, which restores FMRP levels. These results suggest a possible therapeutic treatment to restore FMRP in FXS individuals.

Fragile X syndrome (FXS) is a neurodevelopmental disorder causing a range of maladies including intellectual disability, speech and developmental delays, social deficits, repetitive behavior, attention deficits, and anxiety. Previous studies have shown that an expansion of >200 CGG triplets in the 5′UTR of *FMR1 (Fragile X Messenger Ribonucleoprotein 1)* induces gene methylation and transcriptional silencing, loss of the encoded FMRP, and FXS. FMRP is an RNA-binding protein that interacts with >1,000 mRNAs in the mouse brain and human neurons, predominantly through coding region associations (1–3). FMRP generally inhibits translation and does so by stalling ribosome translocation on mRNAs (4, 5), one of which encodes SETD2, which trimethylates histone H3 lysine 36 (H3K36me3) (6, 7). Elevation of SETD2 in *Fmr1*-deficient mouse hippocampus results in an altered H3K36me3 chromatin landscape in gene bodies, which influences alternative pre-mRNA splicing (6). Many of these mis-splicing events were also detected in human postmortem autism spectrum disorder (ASD) brain and blood tissues (8–12), indicating a convergence of FXS and ASD (6, 13).

We surmised that RNA mis-splicing might be prevalent in human FXS patient tissues (blood and brain) and thus isolated leukocytes from 29 FXS males and 13 typically developing (TD) age-matched males and performed RNA sequencing. Our analysis revealed widespread and statistically robust misregulation of alternative splicing and RNA abundance of >1,000 mRNAs, which might provide readily available, quantifiable, and robust biomarkers for FXS.

Further analysis unexpectedly revealed that *FMR1* RNA was expressed in 21 of 29 FXS leukocyte samples, some nearly as high as *FMR1* transcript levels from TD individuals. This was a surprising result because the *FMR1* locus harboring >200 CGG repeats and full methylation is purported to be silent. However, the highest *FMR1* RNA–expressing FXS individuals were mosaic (CGG repeat number mosaicism or partial methylation of a full expansion). Furthermore, we found that much of the *FMR1* mRNA in the FXS samples was itself mis-spliced to generate *FMR1-217* (ENST00000621447.1), a 1.8 kb isoform comprised of *FMR1* exon 1 and a pseudo-exon within *FMR1* intron 1. This isoform could encode a truncated 31 amino acid polypeptide whose function, if any, is unknown. Further studies are needed to determine whether the *FMR1-217 RNA* or its encoded peptide, if expressed, can mediate toxicity in FXS cells. Additional analysis revealed that *FMR1-217* was detected in FXS dermal and lung-derived fibroblasts as well as in FXS postmortem cortex samples, indicating the preponderance of *FMR1* mis-splicing in FXS populations.

Author affiliations: [a]Program in Molecular Medicine, University of Massachusetts Chan Medical School, Worcester, MA 01605; [b]Department of Pediatrics, Rush University Medical Center, Chicago, IL 60612; [c]RNA Therapeutics Institute, University of Massachusetts Chan Medical School, Worcester, MA 01605; [d]Department of Biochemistry and Molecular Biotechnology, University of Massachusetts Chan Medical School, Worcester, MA 01605; [e]Li Weibo Rare Disease Institute, University of Massachusetts Chan Medical School, Worcester, MA 01605; [f]Department of Neurological Sciences, Rush University Medical Center, Chicago, IL 60612; and [g]Department of Anatomy and Cell Biology, Rush University Medical Center, Chicago, IL 60612

Author contributions: S.S., J.K.W., E.B.-K., and J.D.R. designed research; S.S., K.J.S., and J.K.W. performed research; S.S., K.J.S., J.L., J.K.W., and E.B.-K. contributed new reagents/analytic tools; S.S. and S.R.P. analyzed data; and S.S. and J.D.R. wrote the paper.

Competing interest statement: S.S., E.B.-K., and J.D.R., have filed a patent on RNA-based biomarkers for Fragile X associated disorders. S.S., J.K.W., and J.D.R. have filed a patent on ASO based therapeutics for Fragile X associated disorders.

This article is a PNAS Direct Submission.

[1]To whom correspondence may be addressed. Email: joel.richter@umassmed.edu.

This article contains supporting information online at https://www.pnas.org/lookup/suppl/doi:10.1073/pnas.2302534120/-/DCSupplemental.

Published June 26, 2023.

Fibroblasts from some FXS premutation (i.e., ~55 to 200 CGG repeats) male carriers also express *FMR1-217 RNA*, indicating that mis-splicing may be widespread in other disorders linked to CGG expansions in *FMR1*.

These findings raised the intriguing possibility that modulation of *FMR1-217* mis-splicing might result in increased FMRP levels. Accordingly, we generated eleven 2′-*O*-methoxy ethyl (MOE)/ phosphorothioate-containing antisense oligonucleotides (ASOs) against several regions of *FMR1-217* and transfected them into FXS lymphoblast cells expressing this transcript. A combination of two ASOs blocked improper *FMR1* splicing, rescued proper *FMR1* splicing, and restored FMRP to TD levels. Moreover, application of the DNA methylation inhibitor 5-aza-2′-deoxycytidine (5-AzadC) to a second FXS lymphoblast line as well as FXS fibroblast lines that normally do not express any *FMR1* resulted in the synthesis of both *FMR1* and *FMR1-217* RNAs but little FMRP. However, treatment of these cells with both 5-AzadC and the ASOs produced strong FMRP upregulation. These studies demonstrate that first, in cells from FXS but not TD individuals, a significant proportion of the *FMR1* RNA is mis-spliced to produce the *FMR1-217* isoform. Second, ASO treatment to reduce *FMR1*-217 levels results in FMRP restoration to TD levels. This study provides a basis for further optimizing strategies to reduce the mis-splicing of *FMR1* RNA and may offer a unique therapeutic approach to mitigate FXS using splice-switching ASOs.

Results

Gene Expression Changes in Leukocytes from FXS Individuals. Aberrant splicing of mRNAs is evident in the hippocampal tissue from *Fmr1* KO mice, many of which overlap with those in human postmortem autistic cortex (ref. 6; reviewed in refs. 13 and 14). To investigate whether mis-splicing of mRNAs also occurs in blood samples from FXS individuals, we performed deep (60 to 90 million reads) and long-read (150PE) RNA-seq on freshly obtained leukocytes from 29 FXS males and 13 age-matched typically developing (TD) males (Fig. 1*A*). CGG repeat expansion (>200) for all samples and *FMR1* promoter methylation status for FXS samples when available were confirmed by either southern blot or methylation PCR assays (Dataset S1). Differential alternative splicing (DAS) (15) analysis revealed hundreds of statistically significant events that were altered between genotypes (FXS vs. TD) (using an FDR < 5% and a difference in the exon inclusion levels (PSI, Percent spliced-in) of ≥ 5% (Fig. 1*B* and Dataset S2). A violin plot of the DAS demonstrates that most significant splicing changes were ±~10% in FXS vs. TD with some changes near 30 to 40% (Fig. 1*C*). We confirmed using RT-PCR the increased skipping (~20% in DAS analysis) of exon 3 in the *LAIR2* (leukocyte-associated immunoglobulin–like receptor 2) RNA (Fig. 1*D* and Dataset S2). We also assessed differential gene expression (DGE) and found ~50 RNAs were up- or down-regulated in FXS leukocytes relative to TD (P value < 0.0002) (*SI Appendix,* Fig. S1*A* and Dataset S2) and were clustered based on their z-scores (Dataset S2). *S100B* (S100 calcium-binding protein B), *AGAP1* (ArfGAP With GTPase Domain, Ankyrin Repeat And PH Domain 1), *FAM3B* (FAM3 Metabolism–Regulating Signaling Molecule B), and *RAB25* (RAS oncogene family member 25) are examples of RNAs that were altered in the FXS samples relative to TD (log2FC, P value < 0.0002) (*SI Appendix,* Fig. S1*B*) and confirmed by RT-qPCR (*SI Appendix,* Fig. S1*C*).

Our previous study showed that *Fmr1*-dependent changes in the epigenetic mark H3K36me3 were correlated with aberrant alternative splicing in the mouse hippocampus (6). *Fmr1*-dependent changes in RNA levels were also correlated with H3K4me3 in cultured mouse neurons (16). Consequently, ChIP-Seq was performed to determine whether similar changes in chromatin marks occur in FXS cells. However, results from FXS (n = 2) and TD (n = 3) leukocyte samples showed no genotype-specific changes in H3K36me3 or H3K4me3 (*SI Appendix,* Fig. S1 *D* and *E*). In summary, hundreds of statistically significant events that distinguish between TD and FXS in leukocytes represent robust, unique, and easily obtained biomarkers for human FXS.

***FMR1* RNA Is Expressed and Mis-Spliced in a Subset of FXS Individuals.** Expansion of >200 CGG repeats in *FMR1* induces gene methylation, transcriptional silencing, loss of FMRP, and FXS. It was therefore surprising that in 21 of 29 FXS individuals, *FMR1* RNA isoforms were detected, and in four individuals, the levels were similar to or even higher than those in the TD individuals (Fig. 1*E*, *FMR1* RNA TPM levels). When only full-length *FMR1*–encoding 632 amino acid FMRP (*FMR1-205*) was examined, WBCs from six individuals had levels similar to those of TD (Fig. 1*E*). For comparison, the levels of the *FMR1* paralog *FXR2* were unchanged (Fig. 1*E*). *FMR1* RNA reads were detected at robust levels in TD individuals (blue traces), and also in FXS individuals (coral traces) (Fig. 1*F*). FXS individuals 1-18 expressed relatively high *FMR1* levels (with a cutoff of 0.6 TPM) (H *FMR1*) compared to FXS individuals 19-29 who expressed low or undetectable *FMR1* levels (L *FMR1*) (Fig. 1 *E* and *F*). Remarkably, the H-*FMR1* FXS individuals displayed RNA reads in intron 1 of *FMR1* (black box, enlarged in the panel below, Fig. 1*G*) that were notably absent in TD individuals even though *FMR1* RNA was strongly expressed (Fig. 1*G*). The *FMR1* RNA reads detected in *FMR1* intron 1 correspond to the second exon of the *FMR1*-217 RNA isoform. *FMR1*-217 (ENST00000621447.1) is a 1.8 kb transcript comprised of two exons and is predicted to encode a 31 amino acid polypeptide. Notably, most of the total *FMR1* RNA in the FXS samples is comprised of the aberrantly spliced *FMR1-217* transcript, which is absent in samples from TD individuals (Fig. 1*G* and Dataset S1). TPMs of all 14 *FMR1* isoforms detected in the TD and FXS patient samples are shown in Dataset S1.

Next, we assessed the proportion of full-length *FMR1* RNA to *FMR1*-217 RNA. In the TD samples, 95% of the total *FMR1* RNA (primers Ex1F and Ex1R) represents full-length molecules (primers Ex1F and Ex2R), whereas in the H *FMR1* samples, 75% of the total *FMR1* RNA was full length and 25% was *FMR1*-217 (primers Ex1F and 217R) (*SI Appendix,* Fig. S1*F*). In the L *FMR1* samples, both isoforms were barely detected. The total *FMR1* RNA levels were normalized to *GAPDH* RNA (*P values < 0.05). We confirmed the presence of *FMR1-217* RNA in FXS leukocytes by sequencing the amplified product generated using RT-qPCR [reverse transcription primed with oligodT (*SI Appendix,* Fig. S1*G*). Importantly, all FXS individuals in this study irrespective of *FMR1* expression display typical FXS symptoms which may be due to the negligible amounts of FMRP even in patients with high *FMR1* expression (Dataset S1). Whether *FMR1*-217 or insufficient *FMR1* full-length RNA levels contribute to loss of FMRP in these FXS patients needs further investigation.

Whether *FMR1-217*, or indeed any dysregulated RNA event, contributes to a pathophysiological attribute of FXS is unknown. However, we have investigated whether the parameters we have measured in WBCs are correlated with IQ. Fig. 2 *A* and *B* and Dataset S1 present determinations of methylation status of the *FMR1* gene (by PCR), FMRP levels (ng/μg total protein), CGG repeat number, *FMR1-217*, full-length *FMR1-205* (in TPM) and all detected *FMR1* isoforms (TPM), and IQ (Stanford–Binet test).

As expected, total *FMR1* RNA expression is highly correlated to *FMR1*-217 and *FMR1*-205 isoform expression (Fig. 2*B*). More

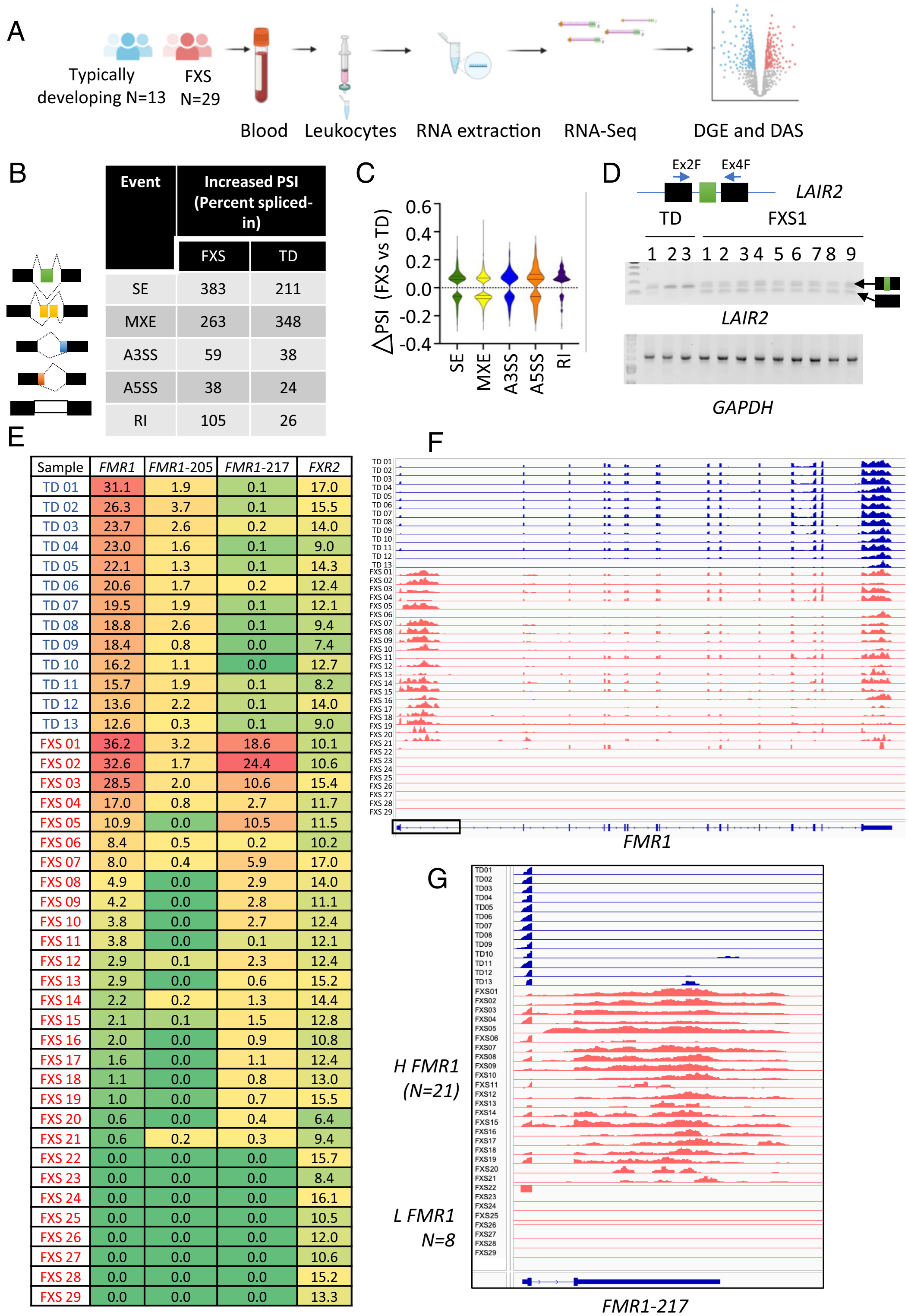

Event	Increased PSI (Percent spliced-in)	
	FXS	TD
SE	383	211
MXE	263	348
A3SS	59	38
A5SS	38	24
RI	105	26

Sample	*FMR1*	*FMR1-205*	*FMR1-217*	*FXR2*
TD 01	31.1	1.9	0.1	17.0
TD 02	26.3	3.7	0.1	15.5
TD 03	23.7	2.6	0.2	14.0
TD 04	23.0	1.6	0.1	9.0
TD 05	22.1	1.3	0.1	14.3
TD 06	20.6	1.7	0.2	12.4
TD 07	19.5	1.9	0.1	12.1
TD 08	18.8	2.6	0.1	9.4
TD 09	18.4	0.8	0.0	7.4
TD 10	16.2	1.1	0.0	12.7
TD 11	15.7	1.9	0.1	8.2
TD 12	13.6	2.2	0.1	14.0
TD 13	12.6	0.3	0.1	9.0
FXS 01	36.2	3.2	18.6	10.1
FXS 02	32.6	1.7	24.4	10.6
FXS 03	28.5	2.0	10.6	15.4
FXS 04	17.0	0.8	2.7	11.7
FXS 05	10.9	0.0	10.5	11.5
FXS 06	8.4	0.5	0.2	10.2
FXS 07	8.0	0.4	5.9	17.0
FXS 08	4.9	0.0	2.9	14.0
FXS 09	4.2	0.0	2.8	11.1
FXS 10	3.8	0.0	2.7	12.4
FXS 11	3.8	0.0	0.1	12.1
FXS 12	2.9	0.1	2.3	12.4
FXS 13	2.9	0.0	0.6	15.2
FXS 14	2.2	0.2	1.3	14.4
FXS 15	2.1	0.1	1.5	12.8
FXS 16	2.0	0.0	0.9	10.8
FXS 17	1.6	0.0	1.1	12.4
FXS 18	1.1	0.0	0.8	13.0
FXS 19	1.0	0.0	0.7	15.5
FXS 20	0.6	0.0	0.4	6.4
FXS 21	0.6	0.2	0.3	9.4
FXS 22	0.0	0.0	0.0	15.7
FXS 23	0.0	0.0	0.0	8.4
FXS 24	0.0	0.0	0.0	16.1
FXS 25	0.0	0.0	0.0	10.5
FXS 26	0.0	0.0	0.0	12.0
FXS 27	0.0	0.0	0.0	10.6
FXS 28	0.0	0.0	0.0	15.2
FXS 29	0.0	0.0	0.0	13.3

Fig. 1. Gene expression changes in leukocytes derived from FXS individuals and identification of a truncated *FMR1* RNA transcript. (*A*) Schematic diagram of leukocyte isolation from fresh blood samples from FXS male (N = 29) and age-matched TD male (N = 13) individuals and subsequent RNA-seq. The data were analyzed for changes in differential gene expression (DGE), and differential alternative splicing (DAS). (*B*) Summary table for changes in alternative splicing events in FXS vs. TD leukocytes detected by rMATS (15) at an FDR < 5% and a difference in the exon inclusion levels (PSI, Percent spliced-in) between the genotypes (deltaPSI) of ≥5%. Schematic for the splicing event categories is shown at the left of the table (see also Dataset S2). (*C*) Violin plots of alternative splicing in FXS vs. TD leukocytes indicating PSI for each type event. (*D*) RT-PCR showing exon 3 skipping of the *LAIR2* RNA in TD (N = 3) and FXS (N = 9) samples. (*E*) Normalized gene counts (transcripts per million, TPM) obtained from RNA-seq data analysis for total *FMR1* (all isoforms), *FMR1-205* (encodes full-length 632 amino acid FMRP), *FMR1-217* (a mis-spliced RNA, see panel *G*), and *FXR2*, a paralog of *FMR1*. The color scale from red to green denotes highest to lowest gene counts. (*F*) IGV viewer tracks of RNA-seq data for FXS and TD individuals for the *FMR1* gene. *FMR1* RNA is detected in all TD individuals (blue) and FXS individuals 1-21 (coral). The black box marked on the *FMR1* gene illustrated at the bottom shows the region of intron 1 with differential reads between TD (1-13) and FXS (1-21) individuals. Expanded view of this region is shown in the bottom. (*G*) An expanded view of the *FMR1* RNA marked with a black box in *G*. The reads map to an exon that comprises the annotated *FMR1*-217 isoform. Sequence data for *FMR1*-217 PCR fragments from FXS RNA sample are shown in *SI Appendix*, Fig. S1*G*. H refers to high and L refers to low *FMR1*.

A

Lab ID	CGG repeat number	Methylation (MPCR)	FMRP [ng / ug total protein]	IQ	*FMR1*	*FMR1-205*	*FMR1-217*
FXS01	140, 175, >200	140 100%, 175 97%, >200 90%	6.56E-03	37.8	36.2	3.2	18.6
FXS02	>200	81%	2.07E-03	26.8	32.6	1.7	24.4
FXS03	150, >200	N/A	N/A	52.0	28.5	2.0	10.6
FXS04	102, >200	N/A	N/A	37.0	17.0	0.8	2.7
FXS05	>200	>200 96%	4.85E-04	35.1	10.9	0.0	10.5
FXS06	65, >200	65 98%, >200 100%	1.77E-02	55.0	8.4	0.5	0.2
FXS07	>200	N/A	2.28E-04	25.0	8.0	0.4	5.9
FXS08	173, >200 (~710,~613)	N/A	N/A	39.9	4.9	0.0	2.9
FXS09	>200	100%	4.40E-04	35.0	4.2	0.0	2.8
FXS10	>200	100%	3.11E-04	56.0	3.8	0.0	2.7
FXS11	>200	100%	6.50E-03	62.3	3.8	0.0	0.1
FXS12	>200	100%	4.85E-04	26.9	2.9	0.1	2.3
FXS13	102, 174, >200	102, 174 100%, >200 100%	5.35E-04	27.6	2.9	0.0	0.6
FXS14	>200	N/A	N/A	20.0	2.2	0.2	1.3
FXS15	>200	100%	2.56E-04	45.9	2.1	0.1	1.5
FXS16	63, >200	63 98%, 194 36%, >200 100%	3.50E-03	53.5	2.0	0.0	0.9
FXS17	>200	100%	1.05E-04	44.0	1.6	0.0	1.1
FXS18	>200	N/A	1.34E-04	30.3	1.1	0.0	0.8
FXS19	>200	N/A	N/A	50.0	1.0	0.0	0.7
FXS20	>200	100%	4.85E-04	29.6	0.6	0.0	0.4
FXS21	>200	100%	2.00E-04	37.7	0.6	0.2	0.3
FXS22	>200	N/A	4.88E-04	35.8	0.0	0.0	0.0
FXS23	>200	94%	N/A	N/A	0.0	0.0	0.0
FXS24	28**, >200	100%	N/A	37.6	0.0	0.0	0.0
FXS25	>200	100%	N/A	N/A	0.0	0.0	0.0
FXS26	>200	100%	4.85E-04	41.8	0.0	0.0	0.0
FXS27	>200	>200 100%	4.85E-04	20.2	0.0	0.0	0.0
FXS28	>200	N/A	N/A	N/A	0.0	0.0	0.0
FXS29	>200	>200: 85%	N/A	49	0	0	0

B

	IQ	*FMR1*	*FMR1-205*	*FMR1-217*	FMRP
IQ	1.00	-0.12	-0.11	-0.25	0.50
FMR1	-0.12	1.00	0.94	0.95	0.30
FMR1-205	-0.11	0.94	1.00	0.82	0.32
FMR1-217	-0.25	0.95	0.82	1.00	0.06
FMRP	0.50	0.30	0.32	0.06	1.00

D

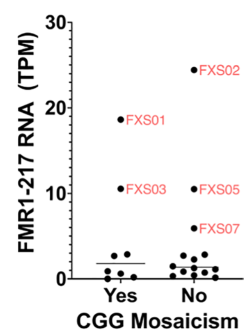

C

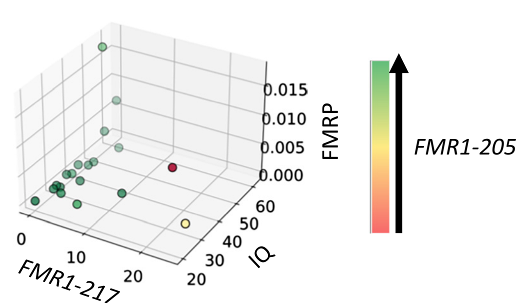

E

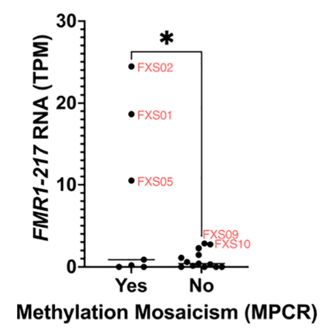

Fig. 2. Correlation of FXS molecular parameters with IQ. (*A*) *FMR1* gene methylation (in percent as determined by PCR analysis, MPCR), FMRP levels (ng/µg total protein), CGG repeat number, *FMR1* (all isoforms, TPM), *FMR1-217* (TPM), and full-length *FMR1-205* (TPM) in leukocytes are listed as well as IQ (Stanford–Binet) for each FXS individual. N/A, not available (see also Dataset S1). (*B*) Correlation coefficients for pairwise comparisons for each parameter (less CGG expansion and methylation) listed in panel *A*. Correlations were based on parameters from 19 FXS individuals because some data were not available from all the 29 samples. (*C*) 3-dimensional comparison of all parameters (less CGG expansion and methylation) listed in panel *A*. The color from green to red represents increasing *FMR1*-205 levels (*A*). The illustration is based on parameters from 19 FXS individuals because some data were not available from all the 29 samples. (*D*) *FMR1*-217 RNA levels (TPM) were assessed between FXS samples with CGG repeat number mosaicism (N = 8) or without (full expansion only) (N = 21). (*E*) *FMR1*-217 RNA levels (TPM) were assessed between FXS samples with methylation mosaicism (N = 7) or without (full expansion only) (N = 13) (**P* < 0.05, *t* test).

intriguing is the moderately positive correlation of IQ with FMRP protein levels. Somewhat surprisingly, *FMR1-205,* which encodes full-length FMRP, has no correlation with IQ. However, we note that while *FMR1-205* encodes the complete 632 amino acid FMRP, other *FMR1* isoforms, which vary in abundance, encode truncated FMRP proteins, whose potential functionality, if any, has not been definitively elucidated. *FMR1-217* has a negative correlation with IQ, perhaps indicating a deleterious effect of this isoform. Fig. 2*C* displays a 3-dimensional comparison of all the parameters noted above. The FXS patients toward the upper end of the IQ range (20 to 60) showed lower *FMR1*-217 levels and higher FMRP levels. Next we assessed the influence of mosaicism (CGG repeat number or methylation) on *FMR1*-217 expression in the FXS patients (Fig. 2 *A* and *D*). Although 38% of the FXS patients (8 of 21) had alleles for both the premutation (55 to 200 CGG repeats) and the full CGG expansion (>200 CGG repeats), the CGG mosaicism did not significantly influence the *FMR1*-217 expression (Fig. 2*D*). The IQ of the patients with or without CGG repeat mosaicism was also comparable (*SI Appendix,* Fig. S2*A*). However, FMRP levels and *FMR1*-205 expression were significantly reduced in patients with no CGG mosaicism (*SI Appendix,* Fig. S2 *B* and *C*), suggesting a reduced capacity of the full expansion alleles to produce FMRP but not the mis-spliced *FMR1*-217 RNA. As expected, the methylation mosaicism was a strong determinant of *FMR1*-217 (Fig. 2 *A* and *E*), FMRP (*SI Appendix,* Fig. S2*B*), and *FMR1*-205 (*SI Appendix,* Fig. S2*C*) expression but not IQ (*SI Appendix,* Fig. S2*A*). These results show several important findings. First, the *FMR1* locus in FXS is frequently transcribed to produce the mis-spliced *FMR1*-217 RNA irrespective of CGG mosaicism and in a few cases when the locus is fully methylated. Second, FMRP levels in WBCs are positively correlated with IQ. Third, the negative correlation of *FMR1-217* with IQ suggests that the process of mis-splicing, the 31 amino acid polypeptide derived from *FMR1-217*, or the *FMR1-217* RNA itself (or all three), might impart some toxic effect manifest in the brain (i.e., IQ). In any event, the levels of *FMR1-217* expression as well as hundreds of additional transcriptome-wide changes in RNA processing events may form the basis for molecular stratification of FXS individuals.

***FMR1*-217 Is Expressed in Human FXS and Premutation Carrier Postmortem Brain.** To investigate whether *FMR1*-217 is expressed in FXS brain, we analyzed publicly available RNA-seq data of postmortem frontal cortex tissues from FXS individuals, premutation carriers (CGG repeats 55-200), and TD individuals (17). *FMR1* RNA (TPM) levels were highest in premutation carriers (Fig. 3*A*). Interestingly, the FXS sample UMB5746, which displays CGG mosaicism, displays high levels of *FMR1* RNA (Fig. 3 *A* and *B*) and to a lesser extent, FMRP (17). Our analysis shows that this individual expressed *FMR1*-217 as did FXS carrier UMB5212, who had fragile X–associated tremor/ataxia syndrome (FXTAS) (Fig. 3 *A* and *B*). Neither TD individual expressed *FMR1*-217 (Fig. 3 *A* and *B*). Thus, *FMR1*-217 RNA may be expressed in the brains of a subset of FXS individuals and premutation carriers.

We find that in FXS individuals with a transcriptionally active *FMR1* gene, *FMR1*-217 is expressed. Next we asked whether demethylating the locus in a transcriptionally silent FXS cell line can result in *FMR1*-217 expression and whether *FMR1* mis-splicing is CGG repeat expansion dependent. We reanalyzed RNA-seq data from Vershkov et al. (18) where the *FMR1* locus was reactivated in transcriptionally silent FXS iPSC–derived neural stem cells (NSCs) by either treatment with 5-AzadC, a nucleoside analog that prevents DNA methylation, or by CRISPR/Cas9 editing to delete the CGG expansion from *FMR1* locus. Reanalysis of these data (Fig. 3*C*) and *FMR1* transcript quantification (TPM) in Fig. 3*D* show reads corresponding to *FMR1-217* (in coral) in the FXS-NSCs upon incubation with 5-AzadC. Moreover, loss of the CGG repeats in the edited cells resulted in no *FMR1-217* reads but instead robust expression of full-length *FMR1*. Total *FMR1* and *FMR1-205* were expressed in the CGG-edited and 5-AzadC-treated cells but not in vehicle-treated cells. This analysis demonstrates that *FMR1-217* is indeed derived from the *FMR1* locus and requires a CGG expansion.

In a complementary study, Liu et al. (19) performed a targeted *FMR1* gene demethylation experiment by incubating FXS iPSC and FXS iPSC–derived neurons with an *FMR1* small-guide RNA and a catalytically inactive Cas9 fused to Tet1 demethylase sequences. Our reanalysis of their subsequent RNA-seq data is shown in (NaN) *MR1* transcript quantification (TPM) in Fig. 3*F*. Their experimental paradigm shows that *FMR1-217* reads are evident only when the gene is demethylated in the FXS cells. Total *FMR1* and *FMR1-205* expression is detected in the Tet1-treated samples (but inexplicably, no *FMR1-205* in sample N1_Tet1). These data therefore show once again that *FMR1-217* is derived from the *FMR1* locus in iPSCs and iPSC-derived neurons and requires a CGG expansion.

To determine whether transcriptome-wide changes in RNA expression could be detected in the frontal cortex, we performed our DGE and DAS analysis of RNA-seq data (17) from the FXS vs. TD (*SI Appendix,* Fig. S3 and Dataset S3) and found statistically significant changes in DGE (*SI Appendix,* Fig. S3*A* and Dataset S3) and DAS events (*SI Appendix,* Fig. S3*B* and Dataset S3). A comparison of FXS samples to FXS premutation carrier samples also shows significant DGE (*SI Appendix,* Fig. S3*C* and Dataset S3) and DAS events (*SI Appendix,* Fig. S3*D* and Dataset S3). Thus, although dataset is small, hundreds of transcriptomic changes are evident in brain tissues from FXS individuals and FXS carriers.

To confirm the expression of *FMR1*-217 RNA in FXS brain tissue, we obtained frozen postmortem cortex samples from six FXS males and five age-matched TD males (UC Davis Health). Using RT-qPCR, we found that the *FMR1* full-length RNA was significantly reduced in the FXS individuals compared to that in the TD individuals. However, 3 of the 6 FXS individuals expressed varying levels of the *FMR1* full-length RNA as well as *FMR1*-217 RNA (1031-09LZ, 1001-18DL, and 1033-08WS) (Fig. 3*G*). Previous studies on the FXS sample 1031-09LZ have noted expression of *FMR1* RNA similar to that in TD individuals, despite the presence of a methylated fully mutated *FMR1* locus (20). However, no detectable FMRP was found in the FXS brain sample 1031-09LZ (21). Also in agreement with our studies, RNA-seq data from Tran *et al* showed no *FMR1* RNA in the FXS tissue samples (1031-08GP and JS03) (Fig. 3 *A* and *B*) as well as an absence of FMRP (17).

To gain greater insight into the relationship of *FMR1*-217 FXS carrier tissue (CGG repeats between 55 and 200), we obtained skin biopsies from three additional premutation carriers and three TD individuals (Fig. 3*H*). The skin samples were cultured in vitro to generate fibroblast cell lines for RNA analysis. Interestingly, using RT-qPCR, we detected *FMR1*-217 in one premutation carrier (C172) with 140 CGG repeats but not in samples with 77 or 98 CGG repeats (Fig. 3*H*). There was no change in total *FMR1* RNA levels among the samples (Fig. 3*H*). Thus, generation of *FMR1*-217 may be linked to the number of CGG repeats in the *FMR1* gene.

ASOs Targeting *FMR1*-217 Restore FMRP Levels in FXS Cell Lines with Partial or Complete *FMR1* Gene Methylation. We next asked whether blocking the formation of *FMR1*-217 could lead to an increase in full-length *FMR1* and concomitantly an increase in FMRP. For these experiments, we used lymphoblast cell lines (LCLs) derived from an FXS individual with a fully methylated locus that is transcriptionally inactive (FXS1, GM07365), an FXS individual with a partially methylated locus that expresses *FMR1* RNA (FXS2, GM06897), and two TD individuals (TD1, GM07174, and TD2, GM06890) (all samples from Coriell

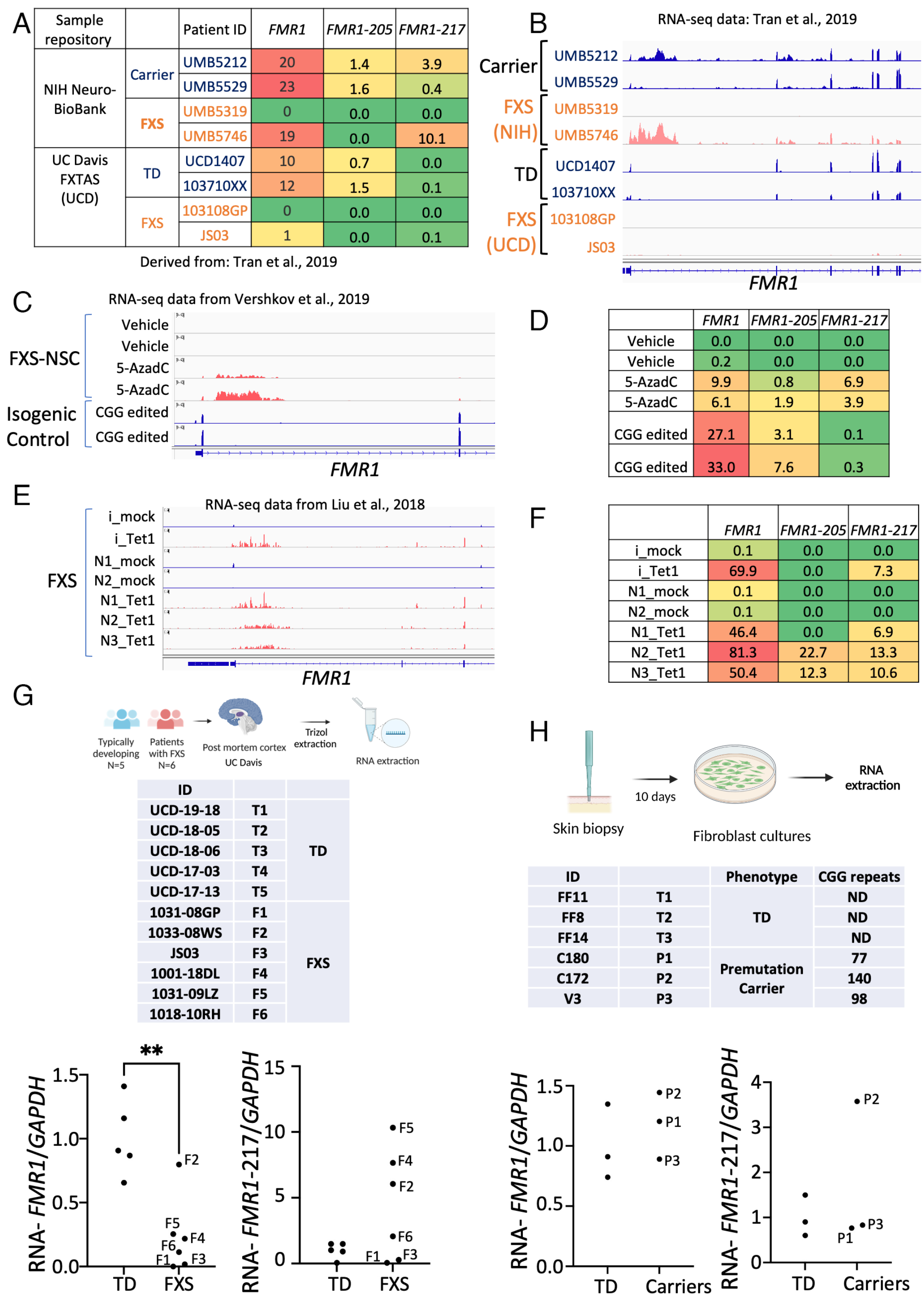

Fig. 3. *FMR1*-217 is derived from *FMR1*, requires the CGG expansion, and is expressed in human postmortem brain tissues (FXS and premutation carriers) and in skin-derived fibroblasts (premutation carrier). (*A*) Sample information for postmortem FXS frontal cortex and premutation FXS carriers and TD individuals (derived from ref. 17). RNA-seq datasets GSE107867 (NIH samples) and GSE117776 were reanalyzed for DGE and DAS. The TPM for *FMR1* RNA in the samples is shown. (*B*) IGV tracks of RNA-seq data (17) for FXS and TD individuals for the *FMR1* gene. (*C*) IGV tracks of selected regions of *FMR1* reanalyzed from the RNA-seq data of Vershkov et al. (18), who deleted the *FMR1* CGG expansion by CRISPR/Cas9 gene editing. Biologic duplicate of iPSC-derived neural stem cells (NSCs) from FXS individuals (FXS-NSC) treated with vehicle or 5-AzadC and isogenic CGG-edited samples are shown. *FMR1-217* reads (coral) are detected only in the 5-AzadC-treated samples. (*D*) Total *FMR1*, full-length *FMR1-205*, and *FMR1-217* reads (TPM) of the samples noted in panel *C* are listed. (*E*) IGV tracks of selected regions of *FMR1* reanalyzed from the RNA-seq data of Liu et al. (19), who performed targeted *FMR1* gene demethylation in FXS iPSCs and iPSC-derived neurons. FXS iPSCs/iPSC-derived neurons incubated a mock guide RNA (blue tracks) (i_mock or N1_mock, N2_mock) or an *FMR1* guide RNA (coral tracks) and Cas9 fused to the Tet1 demethylase (i_Tet1 or N1_Tet1, N2_Tet1, N3_Tet1). (*F*) Total *FMR1*, full-length *FMR1-205*, and *FMR1-217* reads (TPM) of the samples noted in panel *E* are listed. (*G*) Experimental design of RNA extraction from postmortem cortical tissue obtained from six FXS males (F1 to F6) and five TD (T1 to T5) age-matched males. RT-qPCR data for cortical tissue–derived RNA samples representing abundance for *FMR1* and *FMR1*-217 isoforms relative to *GAPDH* RNA. Each sample was analyzed in duplicate. Primers used for amplification are represented in *SI Appendix*, Fig. S1*F* (**$P < 0.01$, *t* test). (*H*) Schematic diagram of fibroblast generated from skin biopsies obtained from three male premutation carriers (P1 to P3) and three male TD individuals (T1 to T3). The table shows patient deidentified designation, genotypes, and CGG repeat numbers in the 5′UTR in the *FMR1* gene. ND, not determined. qPCR data for fibroblast-derived RNA samples representing abundance for *FMR1* and *FMR1*-217 isoforms relative to *GAPDH* RNA are shown. Each sample was analyzed in duplicate. Primers used for amplification are represented in *SI Appendix*, Fig. S1*F* and Dataset S1.

Institute, NJ) (Fig. 4*A*). Western blot analysis shows that modest levels of FMRP are detected in FXS2, but not FXS1 cell lines. FMRP is strongly expressed in TD1 and TD2 cells (ratios of FMRP/GAPDH relative to TD2 are shown below the blot) (Fig. 4*A*). Similar ratios of FMRP protein in these cell lines were obtained by the Luminex Microplex immunochemistry assay (FMRP levels in ng FMRP/µg total protein) (Fig. 4*A*). Using RT-qPCR, we found that *FMR1*-217 RNA is expressed in FXS2 LCLs and comprises 56% of the total *FMR1* RNA compared to only 9% in TD cells (Fig. 4*B*). It is noteworthy that although total *FMR1* RNA levels in FXS2 cells are similar to those in TD cells, FMRP levels are much lower (Fig. 4 *A* and *B*).

Next, we generated eleven antisense oligonucleotides (ASOs) modified with 2′-*O*-methoxyethyl-RNA (MOE) at each nucleotide. The ASOs were tiled across intron 1, the intron 1 and the pseudo-exon junction, or within the pseudo-exon of *FMR1*-217 RNA (Fig. 4*C*), according to standard guidelines for design of exon-skipping ASOs. To test transfection efficiency under the conditions of our experiment, we used a gapmer ASO (80 nM) targeting *MALAT1* RNA (22) for 72 h, which led to ~60% decrease in *MALAT1* RNA levels (*SI Appendix,* Fig. S4*A*). Among the ASOs tested in FXS2 (*SI Appendix,* Fig. S4*B*), the combination of ASO 713 and 714 (80 nM each) led to a significant decrease in *FMR1*-217 and an increase in full-length *FMR1* (Fig. 4*D* and *SI Appendix,* Fig. S4*C*). ASOs 713 and 714 at 80 nM or 160 nM each for 72 h elicited similar decreases in *FMR1*-217 and increases in full-length *FMR1* RNA (*SI Appendix,* Fig. S4*C*). The *MALAT1* ASO had no effect on *FMR1* isoform levels (*SI Appendix*, Fig. S4*C*). Next, we assessed whether FMRP was restored in FXS2 cells following ASO treatment. Fig. 4*E* shows that 80 nM or 160 nM of ASOs 713 and 714 restored FMRP when compared to TD levels. Therefore, ASO treatment of cells from FXS individuals with a transcriptionally active *FMR1* suggests a possible therapeutic path forward through FMRP restoration (Fig. 4*F*).

DNA methylation of the CpG island upstream of the *FMR1* gene promoter in FXS individuals contributes to transcriptional silencing and loss of FMRP. *FMR1* transcription can be reactivated by treatment with 5-AzadC (23, 24) and can result in *FMR1*-217 expression (Fig. 3 *C* and *D*). Consequently, we investigated whether in transcriptionally silent FXS cells, reactivation of *FMR1* using 5-AzadC together with ASO treatment could restore FMRP expression. To do so, the fully methylated FXS1 LCLs were incubated with either 5-AzadC alone or with 80 nM each of ASOs 713 and 714, 24 h prior to the addition of the analog. After 7 d of incubation, the samples were collected and analyzed (Fig. 5*A*). As expected, treatment with the ASOs alone did not affect *FMR1* isoform levels because the locus is completely methylated (Fig. 5*B*). Treatment with 5-AzadC for 1 wk resulted in the expression of *FMR*1-217 and full-length *FMR1* but led to a modest increase in FMRP levels (Fig. 5 *A*–*C* and *SI Appendix,* Fig. S4*D*). A longer treatment time or a higher concentration of 5-AzadC may be needed to further induce FMRP expression. An earlier study shows that a 36-day treatment of FXS LCLs with 5-AzadC restored *FMR1* RNA only up to 40% but produced an even lower level of FMRP compared to that in TD cells (24). Interestingly, a combinatorial treatment of 5-AzadC and ASOs (713 and 714) rescued *FMR1*-217 RNA levels and further increased the full-length *FMR1* compared to 5-AzadC treatment alone (Fig. 5*B*). Although FMRP levels were modestly affected by 5-AzadC alone, a combination of 5-AzadC and the ASOs was more effective in restoring FMRP as compared to that in TD cells (Fig. 5*C* and *SI Appendix,* Fig. S4*D*). These data show that in FXS patient–derived cells with full methylation, a combinatorial treatment of demethylation (5-AzadC treatment) and ASOs may restore FMRP.

Finally, we also incubated two FXS patient–derived fibroblast cell lines with 5-AzadC and the ASOs and determined *FMR1* splicing rescue as well as restoration of FMRP. A dermal cell line from an FXS individual (GM05131b) with CGG repeat numbers of 800,166 (25) and previously shown to harbor a transcriptionally active *FMR1* locus was treated with 5-AzadC and then ASOs 713/714 for 72 h before RNA and protein extraction (*SI Appendix,* Fig. S4*E*). RT-qPCR of *FMR1* and *FMR1-217* shows an ASO-dependent decrease in *FMR1*-217 and a subsequent increase in *FMR1* levels (*SI Appendix,* Fig. S4*E*). The western blot in *SI Appendix,* Fig. S4*F*, shows while 5-AzadC treatment had no effect on FMRP levels, the ASOs alone or in combination with 5-AzadC significantly increased FMRP levels. In a similar experiment with lung fibroblasts from another FXS individual with a fully methylated *FMR1* locus, incubation with 5-AzadC in the absence or presence of ASOs 713/714 resulted in increased *FMR1* and *FMR1-217* (Fig. 5*D*). The western blot in Fig. 5*E* shows that, as with the dermal fibroblasts, ASO treatment resulted in a significant increase of FMRP, albeit lesser than that in the TD fibroblast line.

To summarize, we found that in most FXS patient samples tested, the *FMR1* locus was active but predominantly expressed a mis-spliced *FMR1-217* isoform as well as very modest levels of FMRP. In the FXS cells that are transcriptionally silent, application of demethylating agents induced *FMR1* transcription, which resulted in *FMR1-217* expression. In both cases, treatment of cells with ASOs to block *FMR1*-217 production resulted in partial to complete restoration of FMRP (Fig. 5*F*).

Discussion

Defects in alternative splicing of mRNAs alter the transcript and protein repertoire of cells and occur in neurological disorders such as autism, schizophrenia, and bipolar disorder (8–10). In *Fmr1* knockout mice, hundreds of alternative splicing events were dysregulated (6). Here, we detect >1,000 RNA mis-splicing events in human FXS WBCs. The large number of WBC RNA changes, if correlated with certain pathologies of FXS, might be useful to assess therapeutic outcomes, disease prognosis, and cognitive abilities (11, 12, 26).

When it contains >200 CGG repeats, the *FMR1* gene promoter is methylated and transcriptionally silenced. Surprisingly, we detected *FMR1* RNA in 19 of 29 FXS blood samples and in 5 of 10 FXS postmortem brain samples. Several of these FXS individuals harbor *FMR1* alleles with >200 CGG repeats and are fully methylated. Remarkably, in >70% of these FXS cells and tissues, the *FMR1* RNA is also mis-spliced to generate the *FMR1*-217 isoform, a truncated RNA that could encode a 31 amino acid peptide. *FMR1-217* RNA was not detected in any TD sample. Moreover, in FXS individuals with a fully methylated and silenced *FMR1* locus, abrogation of DNA methylation by 5-AzadC treatment results in *FMR1*-217 expression. *FMR1* mis-splicing to generate the *FMR1*-217 isoform in FXS clearly requires a CGG expansion. For example, *FMR1*-217 RNA expression is detected in FXS premutation carrier–derived fibroblasts with 140 CGG repeats, but not lesser amounts (77 or 98 CGG repeats) or cells from TD individuals (<55 CGG repeats). Further studies are needed to define the interplay between CGG repeat length and possible differential recruitment of splicing factors.

Our data show that although total *FMR1* levels are similar in UFM FXS2 LCLs to that of the TD LCLs, FMRP expression is much lower. Likewise, high *FMR1* expression does not ensure proper FMRP levels in FXS brain tissue samples 1031-09LZ and UMB5746 (17, 21). Similarly, in FXS LCLs and fibroblasts treated with 5-AzadC, a robust increase in *FMR1* RNA, but not FMRP, ensues. Interestingly, all FXS

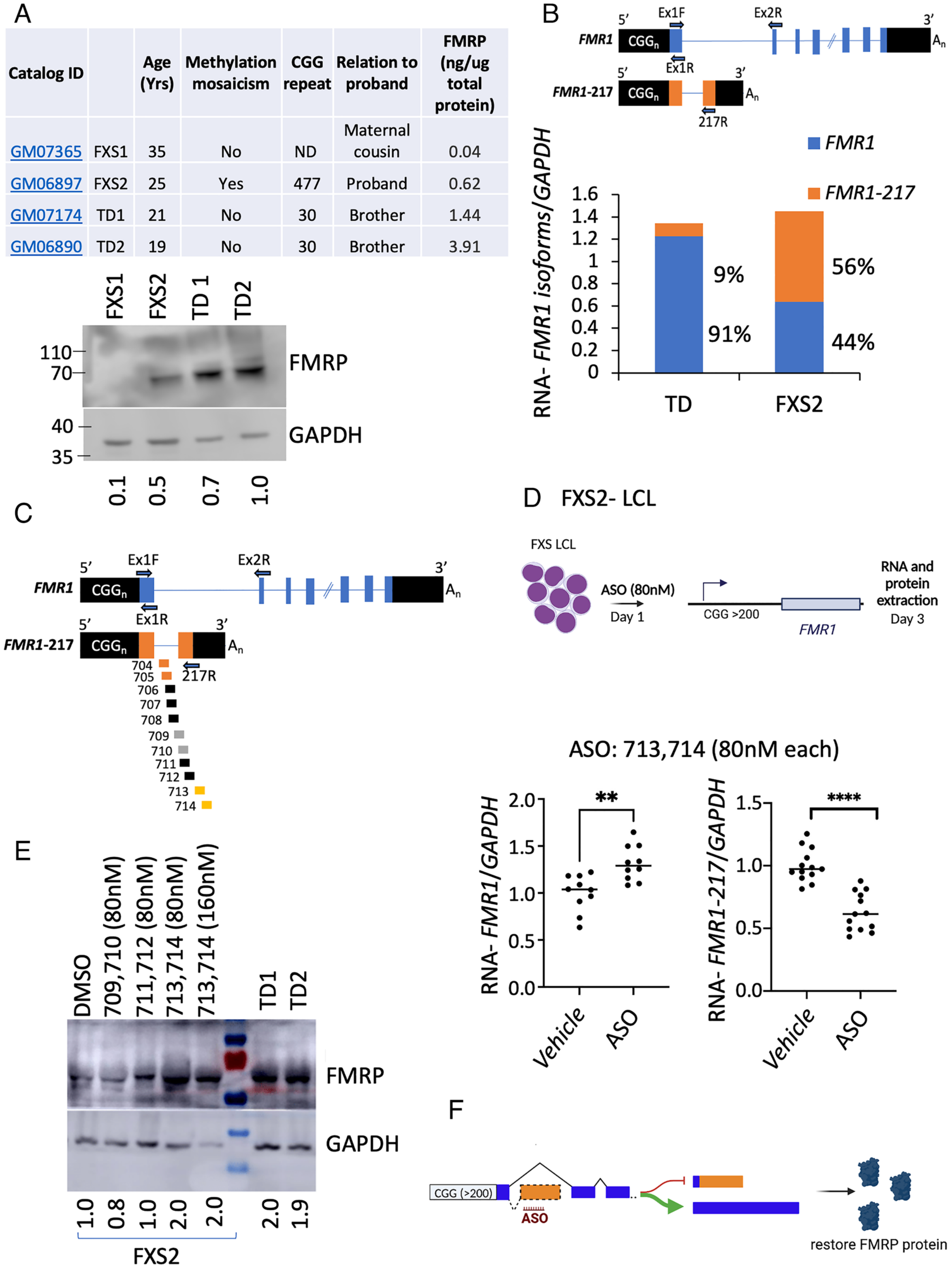

A

Catalog ID		Age (Yrs)	Methylation mosaicism	CGG repeat	Relation to proband	FMRP (ng/ug total protein)
GM07365	FXS1	35	No	ND	Maternal cousin	0.04
GM06897	FXS2	25	Yes	477	Proband	0.62
GM07174	TD1	21	No	30	Brother	1.44
GM06890	TD2	19	No	30	Brother	3.91

Fig. 4. ASOs targeting *FMR1*-217 restore FMRP levels in FXS2 LCLs with incomplete methylation. (*A*) Sample information for lymphoblast cell lines (LCLs) (Coriell Institute, NJ) from two FXS and two TD members of a family is shown. FMRP and GAPDH (loading control) levels were determined by western blots. Ratios of FMRP/GAPDH normalized to FXS1 are shown below the blot. FMRP quantification by Luminex Microplex immunochemistry assay is shown in ng FMRP/μg total protein. (*B*) The proportion of full-length *FMR1* to *FMR1*-217 was quantified using RT-qPCR in the TD and FXS2 LCLs relative to *GAPDH* RNA levels. Primers used for q-PCR are shown in the gene illustration. The total *FMR1* RNA was unchanged, but the proportion of *FMR1*-217 was significantly higher in FXS2 LCL compared to TD LCL. (*C*) ASOs complementary to *FMR1*-217 RNA are illustrated (intron specific: 704 to 706, intron–exon junction specific: 707 to 710 and exon specific: 711 to 714). (*D*) Schematic diagram of the ASO treatment (80 nM for 72 h) of the FXS2 LCLs to determine *FMR1* isoform and FMRP levels after demethylation. DMSO-treated cells were used as a vehicle control (****$P < 0.0001$, **$P < 0.01$, *t* test). (*E*) FMRP levels were determined for FXS2 LCLs treated with DMSO (vehicle) and ASOs as described in Fig. 5*A*. TD LCLs were also probed for FMRP on the same western blots. Ratios of FMRP/GAPDH normalized to FXS1 are shown below the blot. (*F*) Model depicting that ASO-mediated decrease of mis-spliced *FMR1*-217 in FXS2 LCLs can restore *FMR1* full-length RNA and consequently FMRP levels.

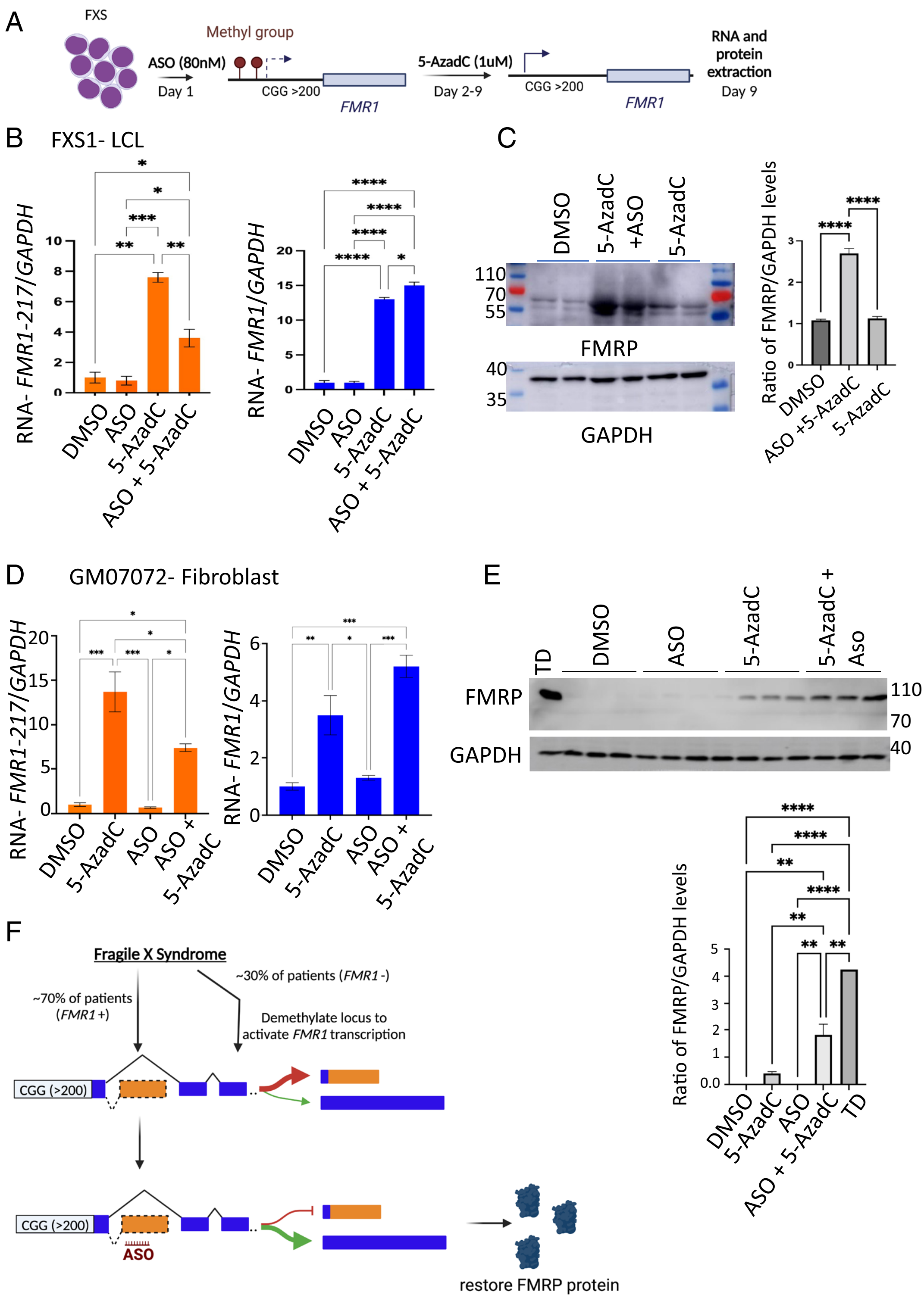

Fig. 5. ASOs targeting *FMR1*-217 in combination with 5-AzadC restores FMRP levels in FXS cells with complete *FMR1* gene methylation. (*A*) Schematic diagram of the fully methylated FXS cells treated with ASOs 713 and 714 (80 nM each) followed by 5-AzadC (1 μM) added on consecutive days 2 to 9 after which RNA and protein were extracted. (*B*) *FMR1*-217 and *FMR1* isoforms were assessed using qPCR primers as shown in *SI Appendix*, Fig. S1*F* and were analyzed using one-way ANOVA with multiple comparisons test (*****P* < 0.0001, ****P* < 0.001, ***P* < 0.01, **P* < 0.05). Data information: bar graphs indicate mean, and error bars indicate ± SEM. (*C*) Western blot of FMRP and GAPDH from FXS1 LCLs treated with DMSO, 5-AzadC, or 5-AzadC plus ASOs. Histogram depicting quantification of western blot for FXS1 cells treated with DMSO, 5-AzadC, and ASO or 5-AzadC alone (N = 3) in arbitrary units. Significance was determined using one-way ANOVA with multiple comparisons test (*****P* < 0.0001). Data information: bar graphs indicate mean, and error bars indicate ± SEM. (*D*) Lung fibroblasts derived from an FXS individual (GM07072, Coriell Institute) were cultured with 5-AzadC for 8 d and then treated with ASOs 713/714 (100 nM each) for 72 h prior to RNA and protein extraction. RT-qPCR analysis of *FMR1-217 FMR1*, and *GAPDH* RNAs in lung fibroblasts treated with DMSO, ASOs 713/714, 5-AzadC, or the ASOs 713/714 plus 5-AzadC. The amounts of *FMR1-217* and *FMR1* were made relative to *GAPDH* (**P* < 0.05, ***P* < 0.01, ****P* < 0.001, one-way ANOVA with multiple comparisons test). (*E*) Western blots of FMRP and GAPDH from the lung fibroblasts treated as in panel *B*. Quantification of FMRP relative to GAPDH is noted below (N = 2) in arbitrary units. Significance was determined using one-way ANOVA with multiple comparisons test (*****P* < 0.0001, ****P* < 0.001, ***P* < 0.01, one-way ANOVA with multiple comparisons test). Data information: bar graphs indicate mean, and error bars indicate ± SEM. (*F*) Model depicting active *FMR1* transcription in FXS cells (or after treatment with demethylating agents to activate *FMR1* transcription) results in the production of mis-spliced *FMR1-217*. Downregulation of *FMR1-217* with an ASO results in rescue of correctly spliced *FMR1* transcripts and restoration of FMRP.

samples that normally express *FMR1* full-length RNA, or after 5-AzadC-mediated transcriptional activation, the *FMR1*-217 mis-spliced RNA is expressed. This relationship between aberrant *FMR1* expression in FXS cells and *FMR1-217* is also evident in FXS iPSC–derived cells. Although our reanalysis of an RNA-seq dataset from FXS neurons with a full CGG expansion shows that *FMR1-217* is not produced, they do so when the *FMR1* gene is specifically targeted for demethylation by CRISPR/inactive Cas9 fused to Tet1 demethylase (ref. 19 and Fig. 3 *E* and *F*). A critical point is that while *FMR1-217* is generated in FXS iPSC–derived NPCs incubated with 5-AzadC, it is not produced when the CGG expansion is deleted by CRISPR/Cas9 (ref. 18 and Fig. 3 *C* and *D*). Therefore, the CGG expansion drives mis-spliced *FMR1-217* generation.

Intellectual impairment is a characteristic of FXS. Our measurements of leukocyte full-length *FMR1-205*, *FMR1-217*, FMRP, and *FMR1* gene methylation allowed us to correlate these molecular parameters with IQ. FMRP was moderately correlated with a higher IQ, whereas *FMR1-217* was weakly correlated with a lower IQ. We considered whether abrogating *FMR1*-217 RNA could elevate *FMR1* and restore FMRP levels. We found that ASOs targeting the second exon of the *FMR1*-217 RNA reduced its levels in FXS cells, rescued full-length *FMR1,* and importantly restored FMRP levels similar to TD cells. Therefore, in a subset of FXS individuals, that express *FMR1-217*, ASO treatment may be a viable therapeutic option. In individuals with a fully methylated *FMR1* locus, an ASO-based treatment would be more complex. Consider that in FXS cells with a silenced *FMR1*, demethylation of the locus by a chemical compound or a demethylating enzyme (18, 24, 27) has met with limited success in restoring FMRP. CRISPR/Cas9-mediated gene editing of the CGG repeats (28–31) has resulted in a nearly 70% restoration of FMRP levels. However, we show that in FXS cells with silenced *FMR1*, DNA demethylation combined with ASO treatment restores FMRP. Therefore, treatments that combine DNA demethylation with a splice-switching ASO might be a useful therapeutic strategy for individuals with a fully silenced *FMR1* gene. In this study, a proof of concept has been presented in which splice-switching ASOs can restore FMRP levels in *FMR1*-expressing FXS cells in vitro. Further studies are needed using neuronal cell cultures or brain organoids to assess this approach. Based on our current work, we hypothesize that *FMR1-217* RNA, which is expressed in FXS human brain tissues as well iPSC-derived neurons, can respond to treatment with splice-switching ASOs and restore FMRP.

Recent advances have shown the clinical feasibility of using ASOs to treat neurological disorders such as spinal muscular atrophy (SMA) (32), myotonic dystrophy (33–35), ALS (amyotrophic lateral sclerosis) (36–40), and Angelman syndrome (41, 42). Our findings suggest that ASOs may be able to correct dysregulated alternative splicing of *FMR1* and restore FMRP in individuals with FXS, thereby offering a unique therapeutic strategy to treat the disorder.

Materials and Methods

Human FXS Participant Studies. FXS male patients (CGG repeats >200) between the ages of 16 to 38 y with FXS phenotypes, IQ range (obtained using the Stanford-Binet Scale–Fifth Edition (SB5) (43) and ABC (The Adaptive Behavior Composite) standard score were measured (Dataset S1). Samples from age-matched TD males (CGG repeats < 55) with a normal IQ and no known neuropsychiatric conditions were obtained (Dataset S1). All participants or their legal guardians, as appropriate, signed informed consent to the study. The project was approved by the Rush University Medical Center's Institutional Review Board. Methylation status was determined using the Asuragen *FMR1* methylation PCR Kit and/or southern blot analysis. FMRP levels were quantified by generating dried blood spots (DBS) or by using peripheral blood mononuclear cell (PBMC) samples. Detailed protocols are available in *SI Appendix*.

Frozen postmortem brain tissues were obtained from the University of California at Davis Brain Repository from FXS male individuals (N = 6) and age-matched TD males (N = 5).

RNA Extraction and Sequencing of Tissue Samples from FXS and TD Individuals.

Leukocytes. Fresh blood (8 mL) was collected (See Dataset S1 and *SI Appendix* section for details), and RNA extraction was performed using the TRIzol™ LS Reagent (ThermoFisher Scientific #10296028). The RNA obtained was then DNase-treated with TURBO™ DNase (Invitrogen #AM2238) and cleaned using the RNA clean and concentrator kit (ZymoResearch #11-325). The quality of RNA (RIN, RNA integrity number >7.3, Dataset S1) was assessed using Fragment analysis. RNA sample (3 μg) was used for directional mRNA library preparation using polyA enrichment (Novogene Co) and the libraries were sequenced on the NovaSeq platform to generate paired-end, 150 bp reads at a sequencing depth of 60 to 90 million reads per sample (Dataset S1).

Brain tissue. RNA was extracted from powdered postmortem frozen cortical tissues using TRIzol™ Reagent (ThermoFisher Scientific # 15596026) and the lysate was collected. Total RNA was extracted using BCP and recovered as above and stored at −80 °C.

ASO Synthesis and Treatment. ASOs were synthesized on a Dr. Oligo 48 synthesizer (Biolytic). 2′-*O*-methoxyethyl (MOE)-modified phosphoramidites were coupled for 8 min. Oligonucleotides were deprotected in concentrated aqueous ammonia (30% in water) at 55 °C for 16 h and characterized by liquid chromatography–mass spectrometry. Final desalting was effected by diafiltration (3× water wash) in a 3-kDa cutoff Amicon centrifugal filter. ASOs were added individually or in combinations to LCL cell lines or fibroblast cultures at a final concentration of 80 nM or 160 nM using Lipofectamine RNAiMAX Transfection Reagent (Thermo Fisher Scientific, 13778030). The cells were collected after 72 h of ASO treatment for RNA and protein extraction.

5-AzadC Treatment. 5-Aza-2′-deoxycytidine (5-AzadC) (Sigma-Aldrich, A3656) was added to the cell cultures (final concentration 1 μM) for 7 consecutive days. For samples with both 5-AzadC and ASO treatment, 80 nM or 160 nM ASOs or vehicle was added on day 1 and either 5-AzadC or DMSO was added each day from day 2 up to day 9 at a final concentration of 1 μM. On day 9, the cells were collected in 1× phosphate-buffered saline to proceed with RNA extraction or western blotting (See *SI Appendix* for further details).

Data, Materials, and Software Availability. All study data are included in the article and/or supporting information. Previously published data were used for this work (GSE117776, GSE112145, and GSE108498) (44–46). All analyses were performed using the DolphinNext platform (47). Datasets generated in this study have been deposited into the Gene Expression Omnibus (GEO) database under the accession number: Super series GSE202179 (48).

ACKNOWLEDGMENTS. The FXS and TD postmortem brain tissues were a gift from Dr. Veronica Martinez-Cerdeno laboratory at UC Davis. We thank Dr. Ozkan Aydemir for help with some of the bioinformatic analysis and Feng Wang (J.K.W lab) for providing reagents and input for the ASO experiments. Schematic diagrams were generated using BioRender. Funding was provided by FRAXA postdoctoral fellowship (to S.S.), FRAXA clinical trial grant (to J.D.R. and E.B.-K.), Simons Foundation for Autism Research Initiative grant (to J.D.R.), NIH grants: R01 GM135087 (J.D.R.), R01 GM046779 (J.D.R.), UL1 TR001453 (J.D.R.), and R01 NS111990 (to J.K.W.), University of Massachusetts Chan Medical School BRIDGE Fund (to J.D.R.), and University of Massachusetts Office of Innovation and Business Development Fund (to J.D.R.).

1. J. C. Darnell *et al.*, FMRP stalls ribosomal translocation on mRNAs linked to synaptic function and autism. *Cell* **14**, 247–261 (2011), 10.1016/j.cell.2011.06.013.
2. T. Maurin *et al.*, HITS-CLIP in various brain areas reveals new targets and new modalities of RNA binding by fragile X mental retardation protein. *Nucleic Acids Res.* **46**, 6344–6355 (2018).
3. M. Li, Identification of FMR1-regulated molecular networks in human neurodevelopment. *Genome Res.* **30**, 361–374 (2020), 10.1101/gr.251405.119.
4. S. D. Sharma *et al.*, Widespread alterations in translation elongation in the brain of Juvenile Fmr1 knockout mice. *Cell Rep.* **26**, 3313–3322.e5 (2019), 10.1016/j.celrep.2019.02.086.

5. T. Udagawa *et al.*, Genetic and acute CPEB1 depletion ameliorate fragile X pathophysiology. *Nat. Med.* **19**, 1473 (2013).
6. S. Shah *et al.*, FMRP control of ribosome translocation promotes chromatin modifications and alternative splicing of neuronal genes linked to autism. *Cell Rep.* **30**, 4459–4472.e6 (2020), 10.1016/j.celrep.2020.02.076.
7. S. Kim, H. Kim, N. Fong, B. Erickson, D. L. Bentley, Pre-mRNA splicing is a determinant of histone H3K36 methylation. *Proc. Natl. Acad. Sci. U.S.A.* **108**, 13564–13569 (2011).
8. M. J. Gandal *et al.*, Transcriptome-wide isoform-level dysregulation in ASD, schizophrenia, and bipolar disorder. *Science* **362**, eaat8127 (2018), 10.1126/science.aat8127.
9. M. Irimia *et al.*, A highly conserved program of neuronal microexons is misregulated in autistic brains. *Cell* **159**, 1511–1523 (2014), 10.1016/j.cell.2014.11.035.
10. M. Quesnel-Vallières *et al.*, Misregulation of an activity-dependent splicing network as a common mechanism underlying autism spectrum disorders. *Mol. Cell* **64**, 1023–1034 (2016), 10.1016/j.molcel.2016.11.033.
11. M. Zafarullah, F. Tassone, Molecular Biomarkers in Fragile X Syndrome. *Brain Sci.* **9**, 96 (2019), 10.3390/brainsci9050096.
12. C. J. Westmark, The quest for fragile X biomarkers. *Mol. Cell. Pediatr.* **1**, 1 (2014) http://www.molcellped.com/content/1/1/1.
13. S. Shah, J. D. Richter, Do Fragile X syndrome and other intellectual disorders converge at aberrant Pre-mRNA splicing? *Front. Psychiatry* **12**, 715346 (2021).
14. J. D. Richter, X. Zhao, The molecular biology of FMRP: New insights into fragile X syndrome. *Nat. Rev. Neurosci.* **22**, 209–222 (2021), 10.1038/s41583-021-00432-0.
15. S. Shen *et al.*, rMATS: Robust and flexible detection of differential alternative splicing from replicate RNA-Seq data. *Proc. Natl. Acad. Sci. U.S.A.* **111**, E5593–E5601 (2014), 10.1073/pnas.1419161111.
16. E. Korb *et al.*, Excess translation of epigenetic regulators contributes to Fragile X syndrome and is alleviated by Brd4 inhibition. *Cell* **170**, 1209–1223.e20 (2017).
17. S. S. Tran *et al.*, Widespread RNA editing dysregulation in brains from autistic individuals. *Nat. Neurosci.* **22**, 25–36 (2019), 10.1038/s41593-018-0287-x.
18. D. Vershkov *et al.*, FMR1 reactivating treatments in Fragile X iPSC-derived neural progenitors in vitro and in vivo. *Cell Rep.* **26**, 2531–2539.e4 (2019).
19. X. S. Liu *et al.*, Rescue of Fragile X syndrome neurons by DNA methylation editing of the FMR1 gene. *Cell* **172**, 979–991.e6 (2018).
20. R. Esanov, N. S. Andrade, S. Bennison, C. Wahlestedt, Z. Zeier The FMR1 promoter is selectively hydroxymethylated in primary neurons of fragile X syndrome patients. *Hum. Mol. Genet.***25**, 4870–4880 (2016), 10.1093/hmg/ddw311.
21. N. Raj *et al.*, Cell-type-specific profiling of human cellular models of fragile X syndrome reveal PI3K-dependent defects in translation and neurogenesis. *Cell Rep.* **35**, 108991 (2021), 10.1016/J.CELREP.2021.108991.
22. M. P. Moazami *et al.*, Quantifying and mitigating motor phenotypes induced by antisense oligonucleotides in the central nervous system. bioRxiv [Preprint] (2021). https://doi.org/10.1101/2021.02.14.431096. Accessed 15 February 2021.
23. E. Tabolacci, F. Palumbo, V. Nobile, G. Neri, Transcriptional reactivation of the FMR1 Gene. A possible approach to the treatment of the fragile X syndrome. *Genes (Basel)* **7**, 1–16 (2016).
24. E. Tabolacci *et al.*, Genome-wide methylation analysis demonstrates that 5-aza-2-deoxycytidine treatment does not cause random DNA demethylation in Fragile X syndrome cells. *Epigenetics Chromatin* **9**, 1–16 (2016).
25. S. D. Sheridan *et al.*, Epigenetic characterization of the FMR1 gene and aberrant neurodevelopment in human induced pluripotent stem cell models of fragile X syndrome. *PLoS One* **6**, e26203 (2011), 10.1371/journal.pone.0026203.
26. E. Berry-Kravis *et al.*, Outcome measures for clinical trials in Fragile X syndrome. *J. Dev. Behav. Pediatr.* **34**, 508–522 (2013).
27. P. Chiurazzi, M. G. Pomponi, R. Willemsen, B. A. Oostra, G. Neri, In vitro reactivation of the FMR1 gene involved in fragile X syndrome. *Hum. Mol. Genet.*, **7**, 109–113 (1998) https://academic.oup.com/hmg/article/7/1/109/637850.
28. J. D. Graef *et al.*, Partial FMRP expression is sufficient to normalize neuronal hyperactivity in Fragile X neurons. *Eur. J. Neurosci.* **51**, 2143–2157 (2020), 10.1111/ejn.14660.
29. J. M. Haenfler *et al.*, Targeted reactivation of FMR1 transcription in Fragile X Syndrome embryonic stem cells. *Front. Mol. Neurosci.* **11**, 282, (2018), 10.3389/fnmol.2018.00282.
30. N. Xie *et al.*, Reactivation of FMR1 by CRISPR/Cas9-mediated deletion of the expanded CGG-repeat of the fragile X chromosome. *PLoS One* **11**, 1–12 (2016).
31. C.-Y. Park *et al.*, Reversion of FMR1 methylation and silencing by editing the triplet repeats in Fragile X iPSC-derived neurons. *Cell Rep.* **13**, 234–241 (2015).
32. R. S. Finkel *et al.*, Treatment of infantile-onset spinal muscular atrophy with nusinersen: A phase 2, open-label, dose-escalation study. *Lancet* **388**, 3017–3026 (2016).
33. S. A. M. Mulders *et al.*, Triplet-repeat oligonucleotide-mediated reversal of RNA toxicity in myotonic dystrophy. *Proc. Natl. Acad. Sci. U.S.A.* **106**, 13915–13920 (2009).
34. S. K. Pandey *et al.*, Identification and characterization of modified antisense oligonucleotides targeting DMPK in mice and nonhuman primates for the treatment of myotonic dystrophy type 1 s. *J. Pharmacol. Exp. Ther.* **355**, 329–340 (2015).
35. T. M. Wheeler *et al.*, Targeting nuclear RNA for in vivo correction of myotonic dystrophy. *Nature* **488**, 111–115 (2012), 10.1038/nature11362.
36. R. A. Smith *et al.*, Antisense oligonucleotide therapy for neurodegenerative disease. *J. Clin. Invest.* **116**, 2290–2296 (2006), 10.1172/JCI25424.
37. C. J. Donnelly *et al.*, RNA toxicity from the ALS/FTD C9ORF72 expansion is mitigated by antisense intervention. *Neuron* **80**, 415–428 (2013).
38. H. Tran *et al.*, Suppression of mutant C9orf72 expression by a potent mixed backbone antisense oligonucleotide. *Nat. Med.* **28**, 117–124 (2022), 10.1038/s41591-021-01557-6.
39. L. A. Becker *et al.*, Therapeutic reduction of ataxin-2 extends lifespan and reduces pathology in TDP-43 mice. *Nature* **544**, 367–371 (2017), 10.1038/nature22038.
40. Y. Q. Jiang, A. Andrade, D. Lipscombe, Spinal morphine but not ziconotide or gabapentin analgesia is affected by alternative splicing of voltage-gated calcium channel CaV2.2 pre-mRNA. *Mol. Pain* **9**, 67 (2013), 10.1186/1744-8069-9-67.
41. C. Milazzo *et al.*, Antisense oligonucleotide treatment rescues UBE3A expression and multiple phenotypes of an Angelman syndrome mouse model. *JCI Insight* **6**, e145991 (2021), 10.1172/jci.insight.145991.
42. S. V. Dindot *et al.*, An ASO therapy for Angelman syndrome that targets an evolutionarily conserved region at the start of the UBE3A-AS transcript. *Sci. Transl. Med.* **15**, abf4077 (2023).
43. G. H. Roid, M. Pomplun, *Contemporary Intellectual Assessment: Theories, Tests, and Issues* (The Guilford Press, New York, NY, ed. 3, 2012), pp. 249–268.
44. S. S. Tran *et al.*, Widespread RNA editing dysregulation in brains from autistic individuals. *Nat. Neurosci.* **22**, 25–36 (2019), 10.1038/s41593-018-0287-x. NCBI GEO (Gene Expression Omnibus), https://www.ncbi.nlm.nih.gov/geo/query/acc.cgi?acc=GSE117776. Deposited 27 July 2018.
45. D. Vershkov *et al.*, FMR1 reactivating treatments in Fragile X iPSC-derived neural progenitors in vitro and in vivo. *Cell Rep.* **26**, 2531–2539.e4 (2019). NCBI GEO (Gene Expression Omnibus), https://www.ncbi.nlm.nih.gov/geo/query/acc.cgi?acc=GSE112145. Deposited 21 March 2018.
46. X. S. Liu *et al.*, Rescue of Fragile X syndrome neurons by DNA methylation editing of the FMR1 gene. *Cell* **172**, 979–991.e6 (2018). NCBI GEO (Gene Expression Omnibus), https://www.ncbi.nlm.nih.gov/geo/query/acc.cgi?acc=GSE108498. Deposited 24 December 2017.
47. A. Kucukural *et al*., DolphinNext: A graphical user interface for creating, deploying and executing Nextflow pipelines. *J Biomol Tech.* **31**, S25 (2020). https://doi.org/10.1101/689539.
48. S. Shah *et al.*, Antisense Oligonucleotide Rescue of CGG Expansion-Dependent FMR1 Mis-Splicing in Fragile X Syndrome Restores FMRP. NCBI GEO (Gene Expression Omnibus). https://www.ncbi.nlm.nih.gov/geo/query/acc.cgi?acc=GSE202179. Deposited 03 May 2022.